Combining Textural Descriptors for Forest Species Recognition

J. G. Martins
Technological Federal University of Parana
R. Cristo Rei, 19,
Toledo, PR, Brasil - 85902-490
Email: martins@utfpr.edu.br

L. S. Oliveira
Federal University of Parana
R. Cel. Francisco H. dos Santos, 100,
Curitiba, PR, Brazil - 81531-990
Email: lesoliveira@inf.ufpr.br

R. Sabourin
Ecole de Technologie Superieure
1100 rue Notre Dame Ouest,
Montreal, Quebec, Canada
Email: robert.sabourin@etsmtl.ca

***Abstract*—In this work we assess the recently introduced Local Phase Quantization (LPQ) as textural descriptor for the problem of forest species recognition. LPQ is based on quantizing the Fourier transform phase in local neighborhoods and the phase can be shown to be a blur invariant property under certain commonly fulfilled conditions. We show through a series of comprehensive experiments that LPQ surpasses the results achieved by the widely used Local Binary Patterns (LPB) and its variants. Our experiments also show, though, that the results can be further improved by combining both LPB and LPQ. In this sense, several different combination strategies were tried out. Using a SVM classifiers, the combination of LPB and LPQ brought an improvement of about 7 percentage points on a database composed by 2,240 microscopic images extracted from 112 different forest species.**

I. Introduction

The field of wood Anatomy has defined a set of primitives to discriminate the vegetable species from which wood can be extracted. Besides the scientific importance, wood identification has a huge practical importance. Wood is a basic raw material applied to make a plenty of products. So, woods can also be categorized by their different applications according to their physical, chemical, and anatomical characteristics, and their prices vary greatly.

Large quantities of wood are transported among short or long distances all over the world. The safe trade of log and timber has become an important issue. Buyers must certify they are buying the correct material while supervising agencies have to certify that wood has been not extracted irregularly from forests. This matter involves millions of dollars and aims at preventing frauds where a wood trader might mix a noble species with cheaper ones, or even try to export wood whose species is endangered.

Nowadays, timber is examined by using the naked eye or sometimes with the aid of a magnifier. In addition to the macroscopic features of wood, physical features such as weight (different moisture content), color (variation), feel, odour, hardness, texture, and surface appearance are also considered. However, identifying an wood log or timber outside of its context (the forest) is not an easy task since one cannot count on flowers, fruits, and leaves. Therefore this task is performed by well-trained specialists but few reach good accuracy in classification due to the time it takes for their training, hence they are not enough to meet the industry demands. Another factor to be taken into account is that the process of manual identification is rather subjective and time consuming. It might lead to diversion of attention as it is a repetitive process and consequently may result in errors, which can become impracticable when checking cargo for export. In this context, computer vision systems become very interesting. In the last decade, however, most of the applications of computer vision in the wood industry were related to quality control, grading, and defect detection [1], [2].

Just recently, some authors began to use computer vision to classify forest species. Tou et al [3] reported two experiments to classify forest species which also use the gray-level co-occurrence matrix (GLCM) features to train a neural network classifier. The authors report recognition rates ranging from 60% to 72% for five different forest species.

Khalid et al [4] presented a system to recognize 20 different Malaysian forest species. A particularity of this method is that the wood samples were first boiled and then cut with a microtome into thin sections. The image acquisition was then performed with an industrial camera of high performance and a LED array lighting. The recognition process is based on a neural network trained with information extracted from GLCM. The database used in their experiments contains 1,753 images for training and only 196 for testing. They report a recognition rate of 95%. A drawback of this strategy is the expensive acquisition protocol which makes it unfeasible for real applications.

Paula et al [5] investigated the use of GLCM and color-based features to recognized 22 different species of the Brazilian flora. In this work they have proposed a segmentation strategy to deal with the great intra-class variability. Experimental results show that when color and GLCM features are used together the results can be considerably improved.

In this work we assess the Local Phase Quantization (LPQ) as textural descriptor for the problem of forest species recognition. LPQ is based on quantizing the Fourier transform phase in local neighborhoods and the phase can be shown to be a blur invariant property under certain commonly fulfilled conditions. Our experiments were performed on a recently proposed database composed of 2,240 microscopic images from 112 different forest species [6]. Such a database is

available for research purposes under request[1].

A series of comprehensive experiments show that the LPQ surpasses the results achieved by the Local Binary Patterns (LPB) and its variants ($LBP^{u2}_{8,2}$, $LBP^{ri}_{8,2}$, $LBP^{riu2}_{8,2}$). In spite of that, we show that the LPQ results can be further improved by combining them with LPB. In this vein, several different combination strategies were tried out along with a SVM classifier. The best results were achieved by fusing the results of the LPQ and $LPB^{ri}_{8,2}$ with the Product rule. Such a combination brought an improvement of about 7.1 percentage points compared to the best results reported in [6].

This paper is structured as follows: Section II introduces the used image database. Section III describes the feature sets we have used to train the classifiers. Section IV reports our experiments and discusses our results. Finally, section V concludes the work.

II. Database

The database used in this work contains 112 different forest species which were catalogued by the Laboratory of Wood Anatomy at the Federal University of Parana in Curitiba, Brazil [6]. As stated before, it is available for research purposes upon request to the VRI-UFPR (http://web.inf.ufpr.br/vri/forest-species-database). The protocol adopted to acquire the images comprises five steps. In the first step, the wood is boiled to make it softer. Then, the wood sample is cut with a sliding microtome to a thickness of about 25 microns (1 micron = 1×10^{-6} meters). In the third step, the veneer is colored using the triple staining technique, which uses acridine red, chrysoidine, and astra blue. In the fourth step, the sample is dehydrated in an ascending alcohol series. Finally, the images are acquired from the sheets of wood using an Olympus Cx40 microscope with a 100x zoom. The resulting images are then saved in PNG (Portable Network Graphics) format with a resolution of 1024×768 pixels.

Each specie has 20 images, totalizing 2,240 microscopic images. Of the 112 available species, 37 are Softwoods and 75 are Hardwoods (Fig. 1). Looking at these samples, we can see that they have different structures. Softwoods have a more homogeneous texture and/or present smaller holes, known as resiniferous channels (Figure 1a), whereas Hardwoods usually present some large holes, known as vessels (Fig. 1b).

Another visual characteristic of the Softwood species is the growth ring, which is defined as the difference in the thickness of the cell walls resulting from the annual development of the tree. We can see this feature in Figure 1a. The coarse cells at the bottom and top of the image indicate more intense physiological activity during spring and summer. The smaller cells in the middle of the image (highlighted in light red) represent the minimum physiological activity that occurs during autumn and winter.

It is worth noting that color cannot be used as an identifying feature in this database, since its hue depends on the dyeing substance used to produce contrast in the microscopic images.

[1]http://web.inf.ufpr.br/vri/forest-species-database

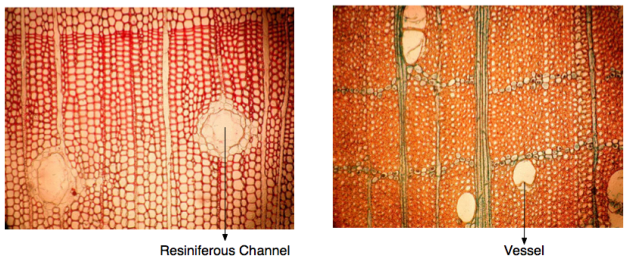

(a) (b)

Figure 1. Samples of the database (a) Softwoods and (b) Hardwoods.

All the images were therefore converted to gray scale (256 levels) in our experiments.

III. Features

In order to make this paper self-contained, in this section we briefly describe both textural descriptors assessed in our experiments, the Local Phase Quantization and Local Binary Patterns.

A. Local Phase Quantization (LPQ)

Proposed by Ojansivu e Heikkila [7], LPQ is based on quantized phase information of the Discrete Fourier Transform (DFT). It uses the local phase information extracted using the 2-D DFT or, more precisely, a Short-Term Fourier Transform (STFT) computed over a rectangular $M \times M$ neighborhood N_x at each pixel position x of the image $f(x)$ defined by

$$F(u,x) = \sum_{y \in N_x} f(x-y) e^{-j2\pi u^T y} = w_u^T f_x \qquad (1)$$

where w_u is the basis vector of the 2-D DFT at frequency u, and f_x is another vector containing all M^2 image samples from N_x.

The STFT can be implemented using a 2-D convolutions $f(x)e^{-2\pi j u^T x}$ for all u. In LPQ only four complex coefficients are considered, corresponding to 2-D frequencies $u_1 = [a, 0]^T$, $u_2 = [0, a]^T$, $u_3 = [a, a]^T$, and $u_4 = [a, -a]^T$, where a is a scalar frequency below the first zero crossing of the DFT $H(u)$. $H(u)$ is DFT of the point spread function of the blur, and u is a vector of coordinates $[u, v]^T$. More details about the LPQ formal definition can be found in [7], where Ojansivu e Heikkila introduced all mathematical formalism. At the end, we will have an 8-position resulting vector G_x for each pixel in the original image. These vectors G_x are quantized using a simple scalar quantizer (Eq. 2, and 3), where g_j is the *j*th component of G_x [7].

$$q_j = \begin{cases} 1, & \text{if } g_j \geqslant 0 \\ 0, & \text{otherwise} \end{cases} \qquad (2)$$

$$b = \sum_{j=1}^{8} q_j 2^{j-1}. \qquad (3)$$

The quantized coefficients are represented as integer values between 0-255 using binary coding (Eq. 3). These binary codes

will be generated and accumulated in a 256-bin histogram, similar to the LBP method [8]. The accumulated values in the histogram will be used as the LPQ 256-dimensional feature vector.

Codes produced by the LPQ operator are insensitive to centrally symmetric blur, which includes motion, out of focus, and atmospheric turbulence blur [9]. Although this ideal invariance is not completely achieved due to the finite window size, the method is still highly insensitive to blur. Because only phase information is used, the method is also invariant to uniform illumination changes [7].

B. Local Binary Patterns (LBP)

The original LBP proposed by Ojala et al. [10] labels the pixels of an image by thresholding a 3×3 neighborhood of each pixel with the center value. Then, considering the results as a binary number and the 256-bin histogram of the LBP labels computed over a region, they used this LBP as a texture descriptor. Figure 2 illustrates this process.

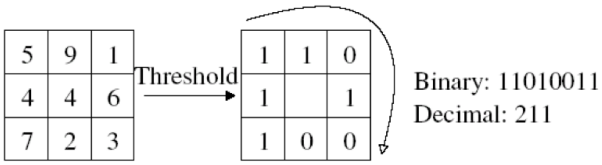

Figure 2. The original LBP operator.

The limitation of the basic LBP operator is its small neighborhood, which cannot absorb the dominant features in large-scale structures. To overcome this problem, the operator was extended to cope with larger neighborhoods. By using circular neighborhoods and bilinearly interpolating the pixel values, any radius and any number of pixels in the neighborhood are allowed. Figure 3 depicts the extended LBP operator, where (P, R) stands for a neighborhood of P equally spaced sampling points on a circle of radius R, which forms a neighbor set that is symmetrical in a circular fashion.

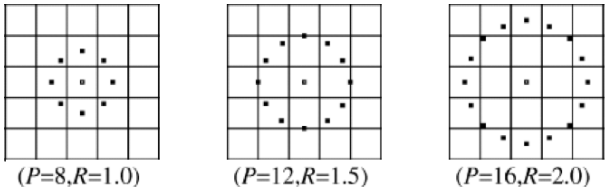

Figure 3. The extended LBP operator [11].

The LPB operator $\text{LBP}_{P,R}$ produces 2^P different binary patterns that can be formed by the P pixels in the neighbor set. However, certain bins contain more information than others, and so, it is possible to use only a subset of the 2^P LBPs. Those fundamental patterns are known as uniform patterns. A LBP is called uniform if it contains at most two bitwise transitions from 0 to 1 or vice versa when the binary string is considered circular. For example, 00000000, 001110000 and 11100001 are uniform patterns. It is observed that uniform patterns account for nearly 90% of all patterns in the (8,1) neighborhood and for about 70% of all patterns in the (16, 2) neighborhood in texture images [10][8].

Accumulating the patterns that have more than two transitions into a single bin yields an LBP operator, denoted $\text{LBP}^{u2}_{P,R}$, with fewer than 2^P bins. For example, the number of labels for a neighborhood of 8 pixels is 256 for the standard LBP but 59 for LBP^{u2}. Then, a histogram of the frequency of the different labels produced by the LBP operator can be built [10].

LBP variants were proposed in [8]. LBP^{ri} and LBP^{riu2} have the same $\text{LBP}_{P,R}$ definition, but they have only 36 and 10 patterns, respectively. LBP^{ri} accumulates, in only one bin (Eq. 4), all binary patterns which keep the same minimum decimal value $LBP^{ri}_{P,R}$ when their P bits are rotated (ROR). LBP^{riu2} combines LBP^{u2} and LBP^{ri} definition. Thus, it uses only the uniform binary patterns and accumulates, in only one bin, those that keep the same minimum decimal value $LBP^{ri}_{P,R}$ when their P bits are rotated.

$$LBP^{ri}_{P,R} = min\{ROR(LBP_{P,R}, i) \;\; i = 0, ..., P-1\}. \quad (4)$$

IV. Experiments and Discussion

The classifier used in this work was the Support Vector Machine (SVM) introduced by Vapnik in [12]. Normalization was performed by linearly scaling each attribute to the range [-1,+1]. The Gaussian kernel was used, with parameters C and tuned using a grid search.

In our experiments, the database was divided into training (40%), validation (20%), and testing (40%). In order to show that the choice of the images used in each subset does not have a significant impact on the recognition rate, each experiment was performed five times with different subsets (randomly selected) for training, validation, and testing. The small standard deviation (σ) values show that the choice of the images for each dataset is not an important issue.

To analyze the data into a multi-class problem, we used the one-against-others strategy, which works by constructing an SVM ω_i for each class q that first separates the class from all the other classes and then uses an expert F to arbitrate between their SVM outputs, in order to produce the final decision. A good reference work listing the multi-class SVM methods is [13].

We used estimation of probabilities to proceed the combination of outputs in order to get a final decision. In this situation, is very useful to have a classifier producing a posterior probability P(class|input). To perform that, we have used the method proposed by Platt in [14]. Here, we are interested in estimation of probabilities because we want to try different fusion strategies like Majority Voting, Sum, Averaging, Product, Max, and Min. A good review about the combination rules can be found in [15].

In the next subsections we i) compare LPQ and LBP^{u2}, ii) assess rotation invariant LPB and iii) show how the combination of LPQ and LPB variants can improve the final results.

A. LPQ and LBP^{u2} features

In this first experiment we compared LPQ with the most used configuration of LBP, the LBP^{u2}. To better assess the impact of these feature sets we trained the classifiers so that both feature sets could be assessed independently. For the LBP^{u2} we tried eight neighbors and different distances, but distance two presented the best results. LPQ was also tested for different window sizes and the best results were achieved using a 3×3-sized window.

Table I shows the best results for each feature set. As we can observe, LPQ surpassed LBP^{u2} in about 3.66 percentage points.

Table I
RECOGNITION RATES FOR LBP^{u2} AND LPQ.

Features	Feature Vector Size	%	σ
LPQ	255	**79.82**	1.34
$LBP^{u2}_{8,2}$	59	76.16	1.09

In order to get a better insight of these results we analyze some classes that have an elevated error rate (between 40% and 65%). Figure 4 shows some samples of these classes.

Figures 4a and 4b show samples of *Picea abies*. For this class of forest species, both LPQ and LBP were able to correctly classify only 50% of the images. In such a case the LPQ performs slightly better since it can deal better with blur (e.g., Figure 4a) than LBP.

Another difficult class is the *Mimosa bimucronata* where the error rate ranges from 40 to 50%. As we can observe from Figures 4c and 4d the same species has quite a different definition of cells and intensity. A similar problem occurs with samples of the class *Eucalyptus grandis*, depicted in Figures 4e and 4f.

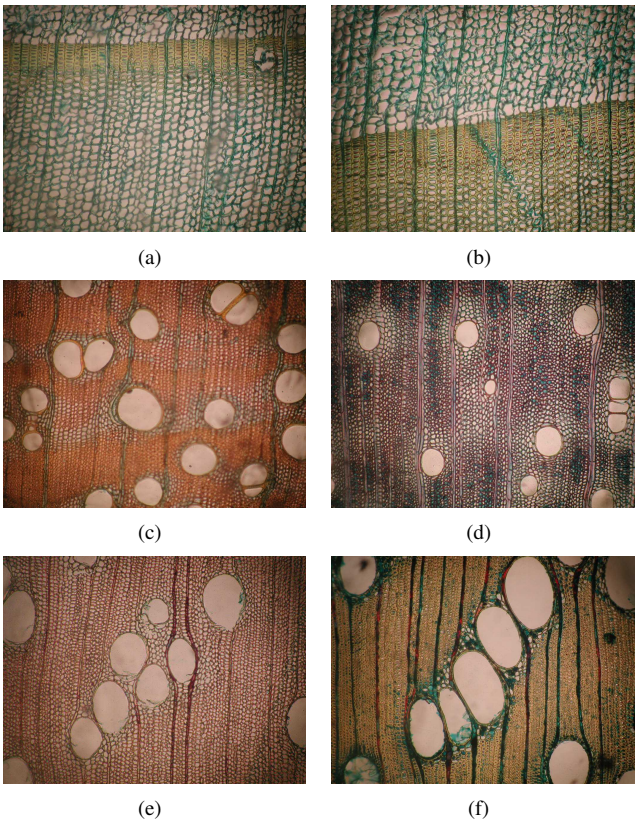

Figure 4. Species with recognition rates lower than 60%: (a-b) *Picea abies*, (c-d) *Mimosa bimucronata*, and (e-f) *Eucalyptus grandis*.

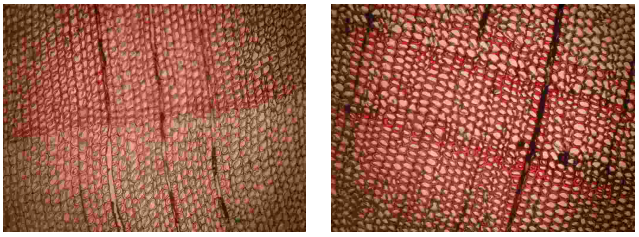

Figure 5. Different angles.

B. Invariance to Rotation

Analyzing the misclassified images, we have just observed differences on their orientations (Fig. 5). These differences are consequence of the slides' displacement on the microscope during image acquisition process. It is important to mention that we did not apply any filter to correct the rotation to the images in our experiments.

Two configurations of rotation invariant LBP were tried out, both of them with eight neighbors and different distances. As reported in Table II, the best results for LBP^{ri} and LBP^{riu2} were achieved for the distance two. $LBP^{ri}_{8,2}$ achieved better results than $LBP^{riu2}_{8,2}$, but both of them were worse than those achieved by traditional $LBP^{u2}_{8,2}$.

We observed that $LBP^{riu2}_{8,2}$ and $LBP^{ri}_{8,2}$ have correctly classified most of those images with differences on their orientation, like the ones shown in Figure 5. However, the overall recognition rate decreased. By analyzing the database, we observed a small number of images with some kind of rotation. Besides LBP^{u2}, LBP^{ri}, and LBP^{riu2} have feature vectors of 59, 36, and 10 components, respectively. So, this impact in the recognition rates could be caused by a loss of representation capability as the number of elements in the LBP feature vector decreases.

C. LPQ and LBP Classifiers Combination

In this last experiment we have combined LPQ and LBP variants using two different strategies. In the first one we

Table II
RECOGNITION RATES FOR $LBP^{ri}_{8,2}$ AND $LBP^{riu2}_{8,2}$.

Features	Feature Vector Size	%	σ
$LBP^{ri}_{8,2}$	36	**75.00**	0.63
$LBP^{riu2}_{8,2}$	10	54.68	1.77

concatenate the LPQ and LPB feature vectors into a single vector. Then, these bigger vectors were used to train the classifiers using the same experimental protocol we have been using so far. Table III shows the recognition rates achieved by such a strategy, where $\oplus$ stands for vector concatenation.

The final feature vectors were composed of 361 components with all four feature vectors concatenated, 315 components for LPQ $\oplus$ LBP^{u2}, 292 components for LPQ $\oplus$ LBP^{ri}, and 266 components for LPQ $\oplus$ LBP^{riu2}. We got an improvement of about 3 percentage points by concatenating the four feature vectors (83.14%, σ=1.78).

Table III
LPQ AND LBP COMBINED THROUGH FEATURE VECTORS JOINT.

Features	**Feature Vector Size**	**%**	σ
LPQ $\oplus$ LBP^{u2} $\oplus$ LBP^{ri} $\oplus$ LBP^{riu2}	361	**83.14**	1.78
LPQ $\oplus$ LBP^{u2}	315	82.72	1.41
LPQ $\oplus$ LBP^{ri}	292	81.80	1.48
LPQ $\oplus$ LBP^{riu2}	266	80.32	1.33

In the second strategy, instead of concatenating the feature vectors we have combined the classifiers' output using the following well-known fusion rules: Majority Voting, Sum, Averaging, Product, Max, and Min. This experiment was motivated after the error analysis when we could observe that the classifiers trained with LPQ and LBP make different mistakes in some cases.

Table IV reports the best result of this experiment. As we can notice, the best result (86.47%) was achieved when combining LPQ and LPB$^{ri}_{8,2}$ through the Product rule. By the way, the Product rule, which is a severe fusion strategy by nature, brought the best results for all the experiments. All four feature sets combined surpassed by 3.3 and 7.1 percentage points the previous combination experiment (feature vectors concatenated) and the best result reported in [6], respectively.

The row Oracle indicates the upper limit for each set of combined classifiers. The Oracle rate is computed considering that the better classifier is always selected. Of course that getting these is not a trivial task and techniques such as dynamic classifier selection can get us closer to the upper limit [16]. In our experiments the best recognition rates were close to the upper limit value. This small difference of 3.8 percentage points shows the effectiveness of combining LPQ and LBP.

V. CONCLUSION

In this work we have exploited two textural descriptors for the problem of forest species recognition. Our results have shown that LPQ surpasses the widely used LPB (and its variants) in all experiments. In spite of the fact that the LBP did not provide the best results, it can not be discard in this kind of application. The combination of LPQ and LPB has been proved effective in improving the overall error rate. Compared with the best results reported in [6], the combination of both feature sets yielded a improvement of about 7 percentage points, achieving a overall recognition rate of 86.47% on a database composed of 112 microscopic images.

Table IV
LPQ AND LBP COMBINED THROUGH FUSION RULES.

Features	**%**	σ	**Combining-Rule**
LPQ, LBP$^{u2}_{8,2}$	77.91	1.09	Maj. Voting
	83.63	0.99	Sum
	83.63	0.99	Average
	84.21	0.86	Product
	81.07	0.83	Max
	74.73	1.25	Min
	86.39	0.90	Oracle
LPQ, LBP$^{ri}_{8,2}$	77.30	0.93	Maj. Voting
	85.54	0.74	Sum
	85.54	0.74	Average
	86.47	0.83	Product
	82.12	1.79	Max
	71.51	0.57	Min
	88.14	1.55	Oracle
LPQ, LBP$^{riu2}_{8,2}$	67.65	1.53	Maj. Voting
	82.52	0.82	Sum
	82.52	0.82	Average
	83.18	0.56	Product
	78.13	1.05	Max
	57.02	2.15	Min
	84.48	1.24	Oracle
LPQ, LBP$^{u2}_{8,2}$, LBP$^{ri}_{8,2}$, LBP$^{riu2}_{8,2}$	80.41	0.59	Maj. Voting
	85.74	0.66	Sum
	85.74	0.66	Average
	85.95	0.83	Product
	81.05	1.41	Max
	53.71	0.98	Min
	90.22	1.20	Oracle

Another point worth of remark is the upper limit of the descriptors considered in this work. As we have seen, if the right classifier is always selected, we could reach 90% of recognition rate. This could be achieved by applying techniques of dynamic selection of classifiers. This is not a trivial task, though, but it sure offers some perspective to build more reliable and robust classification systems.

ACKNOWLEDGMENT

This work have been supported by The National Council for Scientific and Technological Development (CNPq) - Brazil grant # 301653/2011-9 and Coordination for the Improvement of Higher Education Personnel (CAPES).

REFERENCES

[1] L. Thomas and L. Mili, "A robust gm-estimator for the automated detection of external defects on barked hardwood logs and stems," *IEEE Transaction on Signal Processing*, vol. 55, pp. 3568–3576, 2007.

[2] H. Kauppinen, "A two stage defect recognition method for parquet slab grading," *15th International Conference on Pattern Recognition (ICPR'00)*, vol. 4, pp. 803–806, 2000.

[3] J. Y. Tou, P. Y. Lau, and Y. H. Tay, "Computer vision-based wood recognition system," *International Workshop on Advanced Image Technology*, pp. 197–202, 2007.

[4] M. Khalid, E. L. Y. Lee, R. Yusof, and M. Nadaraj, "Design of an intelligent wood species recognition system," *International Journal of Simulation Systems, Science & Technology Special Issue on: Artificial Intelligence*, pp. 9–17, 2008.

[5] P. L. Paula Filho, L. S. Oliveira, A. S. Britto Jr., and R. Sabourin, "Forest species recognition using color-based features," *20th International Conference on Pattern Recognition (ICPR2010)*, pp. 4178–4181, 2010.

[6] J. G. Martins, L. S. Oliveira, S. Nisgoski, and R. Sabourin, "A database for automatic classification of forest species," *Machine Vision and Applications*, 2012.

[7] V. Ojansivu and J. Heikkilä, "Blur insensitive texture classification using local phase quantization," in *Proceedings of the 3rd international conference on Image and Signal Processing*, ser. ICISP '08, 2008, pp. 236–243.

[8] T. Ojala, M. Pietikainen, and T. Maenpaa, "Multiresolution gray-scale and rotation invariant texture classification with local binary patterns," *Pattern Analysis and Machine Intelligence, IEEE Transactions on*, vol. 24, no. 7, pp. 971 –987, jul 2002.

[9] M. R. Banham and A. K. Katsaggelos, "Digital image restoration," *Signal Processing Magazine, IEEE*, vol. 14, no. 2, pp. 24–41, mar 1997.

[10] T. Ojala, M. Pietikinen, and D. Harwood, "A comparative study of texture measures with classification based on featured distributions," *Pattern Recognition*, vol. 29, no. 1, pp. 51 – 59, 1996. [Online]. Available: http://www.sciencedirect.com/science/article/pii/0031320395000674

[11] C. Shan, S. Gong, and P. W. McOwan, "Facial expression recognition based on local binary patterns: A comprehensive study," *Image and Vision Computing*, vol. 27, no. 6, pp. 803 – 816, 2009.

[12] V. Vapnik, *Statistical Learning Theory*. John Wiley and Sons, 1998.

[13] C.-W. Hsu and C.-J. Lin, "A comparison of methods for multi-class support vector machines," *IEEE Transactions on Neural Networks*, vol. 13, pp. 415–425, 2002.

[14] J. Platt, "Probabilistic outputs for support vector machines and comparisons to regularized likelihood methods," in *Advances in Large Margin Classifiers*, A. S. et al, Ed. MIT Press, 1999, pp. 61–74.

[15] J. Kittler, M. Hatef, R. P. W. Duin, and J. Matas, "On combining classifiers," *IEEE Trans. Pattern Anal. Mach. Intell.*, vol. 20, 1998.

[16] A. Ko, R. Sabourin, A. Britto, and L. S. Oliveira, "Pairwise fusion matrix for combining classifiers," *Pattern Recognition*, no. 40, pp. 2198–2210, 2007.